DOI:10.48011/asba.v2i1.1121

Weld Bead Width Measurement in a GMAW WAAM System by using Passive Vision ⋆

Marcus O. Couto * **Ramon R. Costa** * **Antonio C. Leite** **
Fernando Lizarralde * **Arthur G. Rodrigues** ***
João C. Payão Filho ***

* *Electrical Engineering program, COPPE/UFRJ, Rio de Janeiro RJ, Brazil (e-mail: ramon@coep.ufrj.br)*
** *Faculty of Science and Technology, Norwegian University of Life Sciences, Ås, Norway*
*** *Metallurgical and Materials Engineering program, COPPE/UFRJ, Rio de Janeiro RJ, Brazil (e-mail: jpayao@metalmat.ufrj.br)*

Abstract: The development and integration of Wire Arc Additive Manufacturing (WAAM) systems is nowadays a topic of growing interest. Industries are starting to focus on deploying this technology due to its vast capability of producing different types of parts and creating new possibilities for engineering design. Measuring the process characteristics is crucial in a WAAM system, because it helps to ensure that the build up was done according as planned. In this work, it was developed a passive vision-based monitoring method to measure the metal bead width in a WAAM process. The deposition was carried out by using a carbon steel wire with GMAW process, a Motoman HP20 robot arm and a welding torch device. A Xiris XVC-1000 camera was used for visual inspection and mounted in a suitable configuration to minimize arc's noise. The experimental results show that it is possible to measure the bead deposition width in real time with a satisfactory accuracy using monocular cameras. Therefore, it is a feasible solution to be used in WAAM systems with the advantage of being relatively low-cost, as compared to other active vision equipment.

Keywords: Wire arc additive manufacturing; Passive vision; Image processing; Visual sensing; Bead width measurement; Single bead geometry; Metal additive manufacturing.

1. INTRODUCTION

According to Gibson et al. (2010), AM (Additive Manufacturing) is the process of producing 3D objects from a CAD (Computer-Aided Design) without the need of process planning. However, not being as easy as it sounds, AM certainly simplifies the whole process in comparison to other standard manufacturing process that requires a detailed analysis of the part being produced. The parts are built up layer by layer, each layer having a defined thickness, the layer height has a direct impact on the part geometry precision. The thinner the layer the bigger the precision will be achieved, but the production time will also increase.

The junction of a wire feedstock with an electric arc as heat source is referred as WAAM (Wire Arc Additive Manufacturing). It uses standard off-the-shelf hardware, like welding power source, torch, wire feeding system, robot arm and others common welding equipment (Williams et al., 2016). In particular, WAAM has got the attention of industry due its high capability of producing large parts with moderate complexity having a relative high deposition material rate, capability of decrease material waste and consequently environmental friendly characteristics (Wu et al., 2018). However, some challenges rises when using wire as a feedstock, due to the high input heat, deformation caused by residual stress can occur and relative poor accuracy and surface finish also is a problem because its "layer by layer" build up characteristic (Ding et al., 2015b).

WAAM technology works by depositing molten metal layer by layer, it can use different types of power source for melting the wire. Some of the heat energy sources used are Gas Metal Arc Welding (GMAW), Gas Tungsten Arc Welding (GTAW), Plasma Arc Welding (PAW) and Laser Additive manufacturing (Wu et al., 2018; Ding et al., 2011). In Fig.1, a side view representation of the process is shown, a three layers build up is demonstrated using GMAW as the power source for melting the wire. In this case, the material deposition trajectory is done using a robot arm with a constant linear velocity, the image color gradient "red to gray" is used to shown a simplified version of the thermal dissipation considering only the last layer single bead.

⋆ The authors thank Shell Brasil Petróleo Ltda. and Empresa Brasileira de Pesquisa e Inovação Industrial (Embrapii) for funding, and also Agência Nacional de Petróleo, Gás Natural e Biocombustíveis (ANP) by supporting this work.

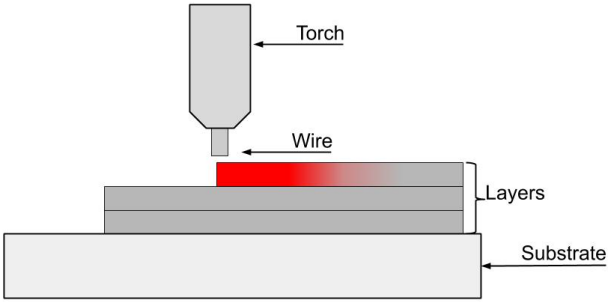

Figure 1. Single wall layer build for a GMAW system.

The basic steps for producing a part using robotic WAAM is shown in Fig.2. First the part is developed and adapted with a CAD software, than 3D slicing is done. The development of the trajectory strategy is done using the layers information after the deposition parameters are established, each layer is covered with a particular designed trajectory. This code is transferred to a robot that will fulfill the planned trajectory, and finally the part is produced, being necessary most of time post-processing to achieve the surface quality and geometric precision specified (Ding et al., 2016).

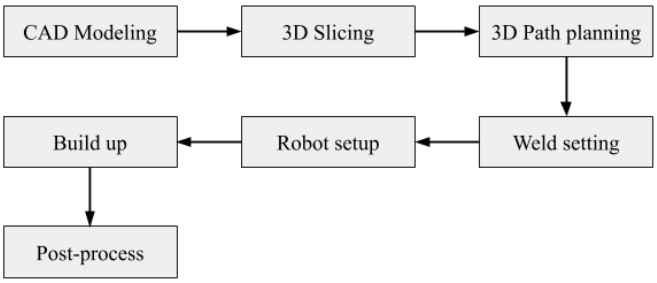

Figure 2. Block diagram for WAAM stages, adapted from Ding et al. (2016)

Currently, mostly of the parts quality assessment relies completely on workers evaluation. To do the inspection they need training and most of time the process consumes a lot of time. Usually the measurements in this step are done using gauges, scales and vision. Vision based inspection methods are commonly used for detecting external defects after welding, many experiments based on vision were done in a lab environment successfully to detect surface defects but not in industry (Chu and Wang, 2016). One of the possible application of Vision sensing and Computer Vision in welding or metal deposition is the development of defect detection system based on the part surface analysis, and also seam tracking in joint welding (Yuan Li et al., 2010).

In Font comas et al. (2017) work, a passive vision system for plasma arc deposition system was developed, tracking the width of the deposited bead. Using a top view layout, the authors also pointed out the possibility of acquiring more information from the image, like the wire feeding angle. Pinto-Lopera et al. (2016) used a single high refresh rate camera to measure the bead height and width, the second being done indirectly by the molten pool measurement. Making a comparison between the measurement done through the camera and a 3D scanner of the bead, achieving good results in the proposed measurement method. Xu et al. (2017) also used passive vision for seam tracking with a GMAW process for ensuring the correct position of the torch during welding. It is possible to notice that passive vision in widely during welding and material deposition. The present work will use passive vision through the usage of a single camera and filters implementation. The acquired raw data is processed, focusing in the width characteristics of the bead geometry, doing a comparison of different methods as well as manual and automatic measurement.

The layer of layer characteristics of WAAM system creates research and development opportunities beyond surface defect inspection. Since the monitoring can be done in every deposited layer, a detection algorithm could be developed focusing on finding internal discontinuities in the deposition, that might turn out to be defects after proper analysis based on standards. In this work, a real-time measurement method based on the combination of passive vision and image processing algorithm will be proposed to estimate the bead width. The accuracy of the vision system will be tested through the deposition of a single bead using a CMT (Cold Metal Transfer), a GMAW variant, with the purpose of validating the weld bead width measurement in a high noisy environment. The proposed vision-based bead width measurement method could be a relative low-cost alternative solution to the conventional active vision equipment such as a 2D non-contact profilometer. Was also noticed the presence of high noise signal during the measurement using passive vision mainly for process like GMAW, one of the application of this work is test two common used filters for smoothing the acquired data during the measurement and compare its performance with a common manual measurement.

2. DEPOSITION SETUP

Cold Metal Transfer (CMT) provides improved stability and lesser spattering, being both important features for Additive Manufacturing. A great advantage of CMT is the ability of providing a uniform bead profile and consequently decrease surface waviness. It also has a lower heat input decreasing part distortion during build up and better mechanical property chances, producing a higher string quality, which is expected for WAAM (Ding et al., 2015b, 2011). Due to these properties the CMT was chosen as the deposition process. The deposition trajectory was done by as 6-DoF Motoman HP20 robot arm (Fig.3) and the welding equipment as well as the camera are both attached to the robot end-effector. The specifications of the HP20 robot arm are: $20\,kg$ payload; $\pm 0.06\,mm$ Repeatability; $1,717\,mm$ H-Reach; $3,063\,mm$ V-Reach; $280\,kg$ Mass; NX100 controller providing best-in-class path planning and collision avoidance/arm interference prevention.

The planned reference path is covered using a constant travel speed. The travel speed (TS) is the linear velocity which the robot end-effector covers the designed path and it is calculated using the x and y axes velocity information, as shown below:

$$TS = \sqrt{V_x^2 + V_y^2}\,. \tag{1}$$

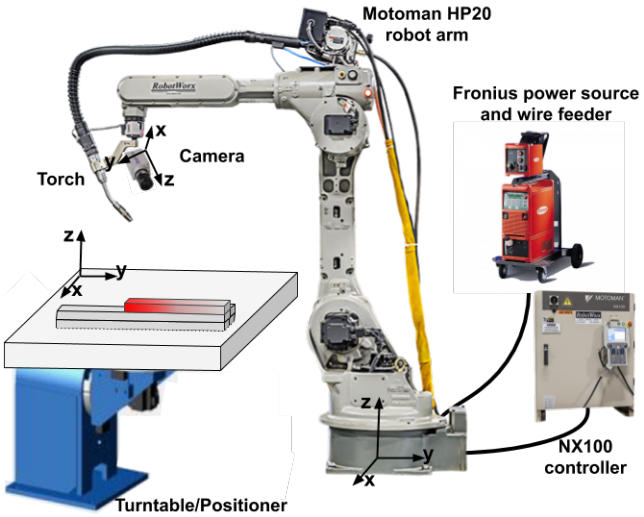

Figure 3. WAAM system: Motoman HP20 robot arm, welding torch, camera and NX100 controller.

For monitoring and acquiring the images during deposition, a regular welding camera from Xiris, model XVC1000 was used (Fig.4) and configured at a distance of $285\,mm$ from the substrate. The specification of the camera are: up to 55 FPS at $1280\,(H) \times 1024\,(V)$ pixels; lens with $16\,mm$ focal distance; $6.8\,\rho\,m$ square pixel; $998\,\rho\,m$ exposure time. However, any other camera with proper specification for capturing welding and deposition images by electric arc could be used.

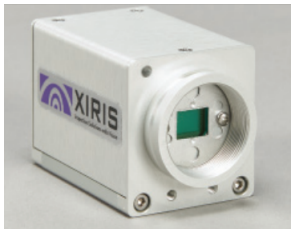

Figure 4. Xiris XVC-1000 camera.

A schematic example of a wall being deposited by layers can be seen in Fig.5. The color gradient used in the last layer represents deposited bead glowing due to its high temperature. The camera is focused in the material being deposited, right after the metal pool in the opposite direction of movement. The light emitted by the bead in this area is high and this characteristic is used for detecting the toe of the bead being deposited. The thermal dissipation were also represented by this gradient only in the last layer deposition for simplicity, with red and gray representing the highest and lowest temperature respectively. Both welding torch and camera are attached to the robot arm, which guides them through the planned path with a constant linear velocity of $TS = 8\ mm\,s^{-1}$. One set of single beads deposited during the deposition step can be seen in Figure 6, being also used for the development of the monitoring width algorithm.

3. WELD BEAD AND LAYER DESIGN

Finding a relation between the deposition parameters and the single bead geometry is very important in a

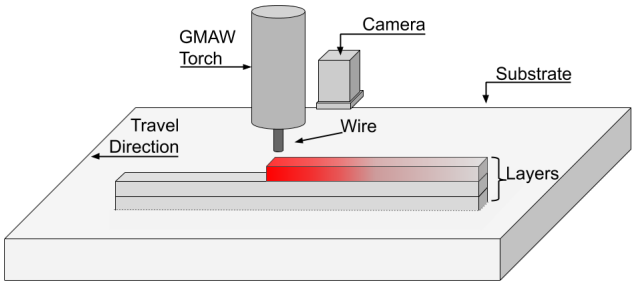

Figure 5. Deposition and visual monitoring schematic.

Figure 6. Single bead sample

WAAM system. Many researches had gone towards this subject, with different mathematical models being used to describe the bead geometry. The three most commonly used functions are the parabola, cosine and arc. Overall, it has been concluded that the bead profile is largely dependant of the wire feed rate and the travel speed (Ding et al., 2015a).

The deposit bead profile can be seen in Fig.7 with its main characteristics, wherein by using a suitable camera mounted in the current configuration (i.e., facing the substrate) is only possible to extract the width information. However, it is also possible to estimate other process features, such as the bead height and the weld pool geometry mounting the camera respectively facing the layer build up laterally and the weld pool directly.

The current work will focus on acquiring the bead width information constantly and map its variation frame by frame, during the single bead deposition.

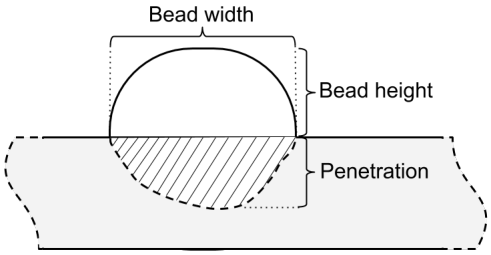

Figure 7. Cross-section profile of the bead.

Information about the bead width being deposited can be considered one of the most important variables on the weld bead geometry when the surface quality of the layer deposited is being the focus. Its dimension depends on other variables such as travel speed and wire feed speed.

A constant bead width within the design planning during all layer deposition, results in lesser waste of material and a better fit and finish of the deposition (Cruz et al., 2015).

3.1 Surface layer quality

In AM, a layer can be built by depositing many single weld beads side by side (Ding et al., 2015a). In Fig.1 and Fig.5 it can be seen that the current layer is deposited over the previous deposited layer surface. As the previous layer is used as base for a new layer, the surface quality of every layer becomes very important to increase the precision and avoid possible defects.

Surface quality, in other words, can be considered how smooth is the surface of each layer. In multi-side beads scenario, the cross-section overlapped between single bead has great influence on the surface quality and dimension accuracy Xiong et al. (2013a). Two overlapping models have been used to show the interaction of side beads and ensure a better surface quality in a multi-bead overlapping process: the Flat Overlapping Model (FOM) (Xiong et al., 2013a) and Tangent Overlapping Model (TOM) (Ding et al., 2015a), represented in Fig.8 and Fig.9, respectively.

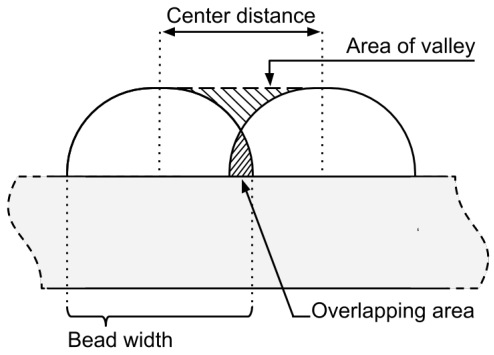

Figure 8. Flat overlapping model, adapted from Xiong et al. (2013a).

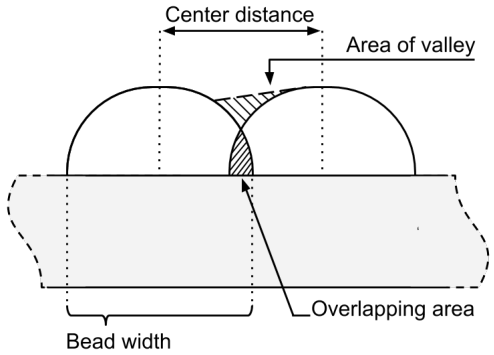

Figure 9. Tangent overlapping model, adapted from Ding et al. (2015a).

The aforementioned FOM and TOM overlapping models proposed an optimum value for the distance between the center of each adjacent bead, being described as center distance (d) in Fig.8 and Fig.9, in which the "Area of valley" will be equal to the "Overlapping area", improving the surface quality in layers manufacturing using arc. In Xiong et al. (2013a), the authors propose that an optimal distance between adjacent beads have a direct relation with the width, achieving the relation: $d = 0.667w$. Ding et al. (2015a) also proposed the same relation between the center distance and the bead width arriving at a similar linear relation $d = 0.738w$, with w being the weld bead width. A comparison between both models in a manufactured wall with five layers can also be found in the work done by Ding et al. (2015a). Thus it is possible to conclude that the bead width tracking is very important for high-quality additive manufacturing system, due to the fact that its layer surface finish is directly related to the weld bead width. Being capable of measuring constantly this characteristics highly improves the capability if ensuring the quality and accuracy of the deposition process. In Fig.10, it is possible to check how a well planned distance between the centers influence the quality of the surface as well as the geometry accuracy of the material deposited. The overlapped area must be equal to the area of the valley for achieving good results.

(a) $d \geq w$, no overlapping

(b) $d < w$, overlapping area smaller than area of valley.

(c) $d < w$, overlapping equals to area of valley.

(d) $d << w$, overlapping area bigger than area of valley.

Figure 10. Overlapping area influence over surface quality, adapted from Xiong et al. (2013a).

4. VISION IN WELDING AND WAAM

In welding, vision is used to gather information of the molten pool and the weld bead. This information is used for tracking, guiding and feed backing to the controller, and it can be divided in two types, the passive and active groups, which are classified according to the image light source used (Chen et al., 2004; Wu and Chen, 2007). A reliable monitoring system is a key aspect of quality assurance during an additive manufacturing process. By analyzing the characteristics of the deposition, if we can guarantee that the buildup was done according to what was planned, then it is possible to decrease the probability of defects in the manufactured part. Moreover, mapping the bead geometry, mainly the bead width along the

reference trajectory, can also help the inspection stage. Deposited areas where the geometry is not according to the specifications have bigger chance of presenting defects and could be tracked during the inspection.

Active vision sensing requires an internal light source, for example a laser or other assistance light for the process to be monitored. In welding, active vision sensing is used to restrain the welding arc interference, however it is expensive to be applied in a common welding process. On the other hand, passive vision works without the assistance of a light source, using only the energy provided externally, in this case by the self-arc welding region. It requires the implementation of filters to wipe off disturbances the data (image) which is gathered through the sensor – by using light source from the arc is subject to a high level of noise. Passive vision is considered a practical way of monitoring weld pool characteristics and it is also cheaper than active vision, being preferred for monitoring and control welding processes (Wu and Chen, 2007). At the work published by Xu et al. (2017), the authors also considered passive vision a cheaper solution and it provides enough information about the environment which can overcome the problem of tracking systems based on laser sensors (Xu et al., 2014).

Most of the quality control procedures in welding processes are done after the work is finished, however, in WAAM processes this characteristics can be expanded. Since the part is build up from scratch, it creates a number of research and development opportunities for monitoring the whole process, layer by layer. Indeed, as mentioned before, the design and development of a monitoring system suitable for WAAM processes has proved to be very important. Enabling defect detection, ensuring build up parameters and also enabling feedback control of parts of the process are relevant assets for next generation of WAAM systems. In this context, vision sensing and computer vision have enabled the development of surface defect detection applications. Typical application examples come from circuit board inspection, surface defect recognition and classification, seam tracking, deposit bead profile monitoring and other inspections stages (e.g., alignment, positioning) (Yuan Li et al., 2010).

However, extracting and monitoring bead characteristics using vision sensing is a challenging problem due to the presence of uncertainties, external disturbances and process noise. WAAM by nature is a very complex process subject to many types of uncertainties and disturbances that can be considered, such as surface non-uniformity, the arc itself, the material used in the substrate due its high reflexiveness, and the wire quality. The working environment itself can also be considered as a source of variations and some factors contribute to the noise generation, such as the cable line, jigs and change in light conditions. All of these factors increase the difficulty for the computer vision system and must be considered when developing processing image algorithms with any robustness properties (Chen et al., 2007).

5. MONITORING SYSTEM FOR WAAM

Since the overlapping degree is directly impacted by the step-over distance between side beads, monitoring the weld bead width shows a very important task in this technology. It allows a constant reading of the width variation during the deposition and make possible to check if the overlapping area in a defined position is according with the specification planned. Improving the quality of the layer deposited and also decreasing the probability of internal defects, such as lack of fusion and voids.

However, as previously mentioned, the environment is highly noisy and full of disturbances due to the process characteristics and it cannot be easily attenuated. It is possible to decrease the noise levels by the use of standard welding screen protections, change in the camera configuration and digital image processing filters. All these details must be studied and configured during the assembly, test and development of the algorithm. In Fig. 11 it is possible to observe the example of two frames captured by the monocular camera during the deposition of the single bead.

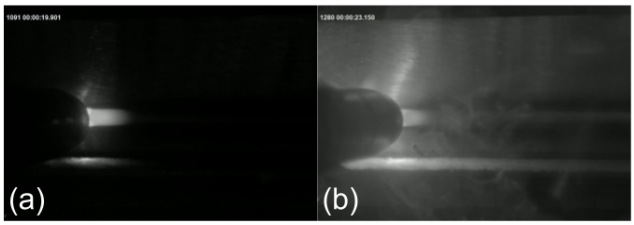

Figure 11. First and second frames capture by the camera.

These frames represents well the dynamic change in the contrast between distinct frames, being directly related to the arc-generated light and also can be considered as process noise. Other characteristics that increases the level of difficulty of extracting information through vision can be noticed in Fig. 11(b), the fumes, that creates another challenge for the vision system handle.

In this scenario, the following steps will be used to treat the CMOS camera data being captured and extract features from it. The testing and development of the image processing algorithm used in this work was done using an Intel Core I5-6300HQ processor. The development of the algorithm was done using ROS (Robot Operating System) framework for better integration with the robot.

Figure 12 describes the stages for the image processing algorithm. At step 1, the camera used captures the image in gray-scale format. However, the data is captured in a 3D

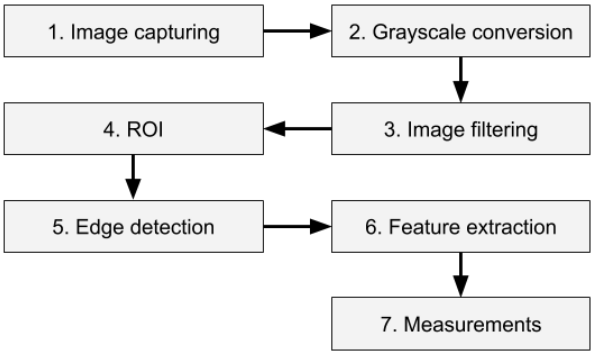

Figure 12. Image processing stages. ROI: Region of interest

array by the algorithm. Step 2 converts the data to a 2D array using gray-scale conversion, for this specific camera used selecting one of the three array would show the same result, however, using gray-scale conversion makes the algorithm more adapted to other types of camera that might be used and could capture the image in RGB format.

The image captured comes with a lot of noise due to the process characteristics and smoothing it is very important to decrease the noise level creating a more uniform image. Three noise reduction filters (step 3) were tested, gaussian, median and non-local means (Buades et al., 2011), the computational cost of the non-local means is a lot bigger than the other two, it took 0.54 s to complete the operation while the gaussian took 0.0008 s and median 0.0029 s. The non-local means filter presented a better result when compared with the median and gaussian, however, had great impact on the algorithm performance even when used under a small region. Therefore, for the filtering step it was chosen to use the gaussian filter with a 5x5 mask size. It had similar results removing noise when compared to the median filter but maintained a good sharpness level while having a lower computational cost.

To decrease computational costs the filter and all image processing were applied inside the ROI (region of interest). The region of interest was placed near the torch for better identification due to deposit bead heat light intensity with a 30 pixels x 110 pixels size . This configuration helps the detection of the edges, guaranteeing a higher intensity gradient transition in the edge detected pixels.

Step 5 is responsible for edge detection, edges are detected by the intensity changes in the image, first or second order derivative are used to accomplish the detection. The image gradient (equation 2) is broadly used for edge detection, it has the function of highlighting the transition between different intensities in mapped pixels. The gradient, are the representation of the image first derivative and are applied on the image by using masks with specific dimension and weight. The result is a vector pointing in the direction of greatest rate of change. Magnitude operation (equation 3) is used to find the rate of change at every location pixel analysed. It returns the rate of change value of the intensity. Being constantly used for edge detection algorithms (Gonzalez and Woods, 2007). Canny algorithm (Canny, 1986), was used for edge detection in the present work, it had a good result, retrieving sharp edges and having low noise level. It presented a better result for this application when compared with other edge detection algorithms, such as Sobel, Laplacian and Scharr.

$$\nabla f = grad(f) = \begin{bmatrix} g_x \\ g_y \end{bmatrix} = \begin{bmatrix} \frac{\partial f}{\partial x} \\ \frac{\partial f}{\partial y} \end{bmatrix} \tag{2}$$

$$M(x, y) = mag(\nabla f) = \sqrt{g_x^2 + g_y^2} \tag{3}$$

After extracting the edge with Canny edge detector, the data obtained is an image with a point cloud area. To find out if a subset of these points lies in the same line, the Hough line transform algorithm was used. A

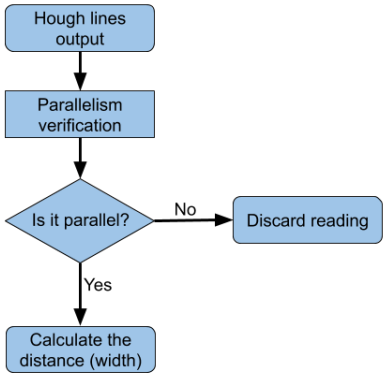

Figure 13. Lines parallelism verification steps for width measurement

polar representation (equation 4) is used, avoiding the parameters approaching infinity in some particular cases. The algorithm will test each point with a set of lines and consider a valid line the one that has a certain amount of points above its path. Hough transform has a strong anti-noise ability and good detection with low signal to noise ratio (Xiong et al., 2013b). The algorithm took around 246 μs to complete the line detection, having a low computational cost and also being feasible for usage in a real-time detection system.

$$\rho = x \cos\theta + y \sin\theta \tag{4}$$

The bead width is calculated using the distance between both detected edges. Both edges are now represented by the output of the Hough transform algorithm is line represented as a vector in polar coordinate. Before finding the distance between the lines the algorithm verifies the parallelism between every line identified and calculate it only if the angle difference is inside a defined threshold, otherwise the operation is discarded. A simple flowchart for this verification step can be seen in fig.13 representing the verification logic.

However, not always the algorithm is capable of extracting the features, as established previously, the image has a lot of noise due the process used. The light intensity is constantly changing due to arc's short circuiting, making detecting problematic for the algorithm on every received frame. To work around this characteristic, filtering the data was necessary with a "Buffer filter", as called in this paper, it was designed to do outlier rejection and handle data loss.

This filter was designed as a vector with n positions, this dimension is adjustable by the user. The filter optimum dimension must be reached through testing, for reaching a good balance in precision of the measurements and data filtering. The data in the filter is organized in a queue format, the newest message occupies the first position in the vector and the last message is discarded. In this work the dimension used in the buff filter was 15.

The Buffer Filter uses the vector's mean value as a threshold for new messages received, when the the data received is above the threshold the data is considered valid and when its below it is discarded and the first position of the vector now will assume empty as value,

meaning that no width information was received. The video is showed to the user with the edge detection happening, see fig.14, it also represents two distinct frames showed to the end user with the edge detection running inside the region of interest.

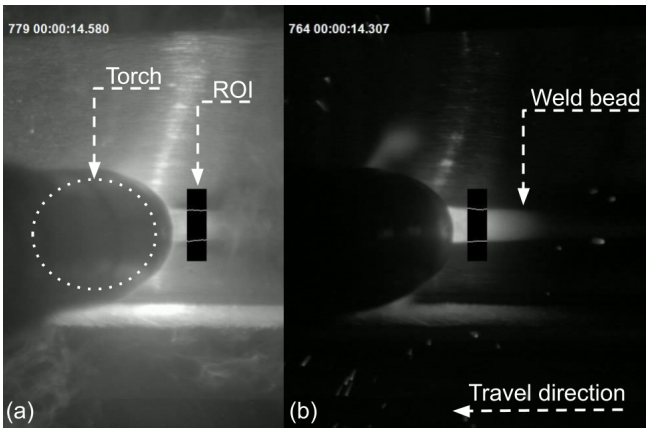

Figure 14. Monitor video with edge detection

Both images are good to demonstrate the difference between distinct captured frames during the material deposition. In fig.14(a) it is possible to see a lot of fume coming from the molten pool area, and in fig.14(b) a lot of spatter. Both area considered noise in the system.

The information is mapped and recorded in every frame during all deposition process. It was possible to gather information of the width constantly and with low variance as can be seen in Fig.15. However the raw data is obtained with a lot of noise and two filters were added to smooth the information. The median filter is represented by the red line and the low-pass band filter is represented by the blue lines. Both had adequate performance in filtering the noise, with the low-pass having better signal-to-noise ratio but a longer settling time when compared with the median filter.

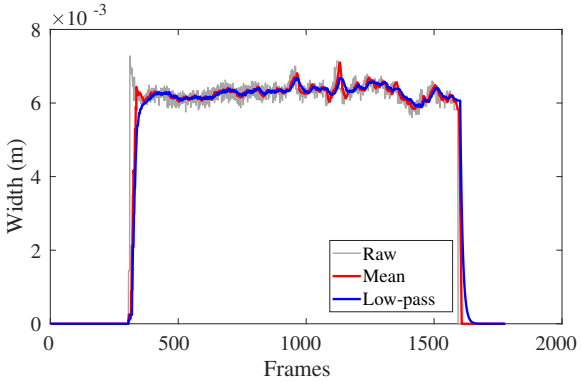

Figure 15. Bead width monitoring plot

A comparison between the mean and low-pass algorithm filtered measurements and a manual measurement by software, shows a deviation of 1% from both measurements. The mean measurement from both filters output were $6.27mm$ and from the manually measurements were $6.24mm$ when done in specific points of the bead. The algorithm output data is much more rich with information due to the fact that it monitors the bead through all the planned deposition path. Figure 16 it is shown how the manually measurement was done through an image software.

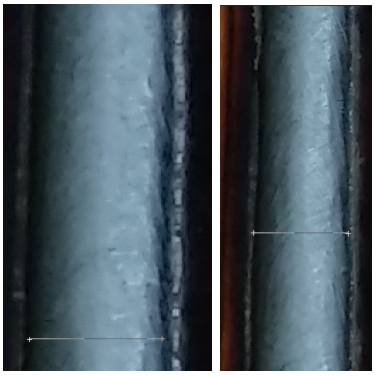

Figure 16. Manual measurements of the bead width

6. CONCLUSIONS

As showed in the present work monocular cameras are capable of extracting important information of the deposition, with a proper image processing algorithm, and are also an important visual monitoring device for the operator. It is a great option for development and implementation in real-time monitoring system for a WAAM system.

The width monitoring was done successfully, even under a high noisy deposition process. In particular the short circuit characteristic generates a lot of problems in the acquired image, saturating and also decreases the intensity rate between pixels. However, with the use of a Buffer filter it was possible recording previous states and rejecting outliers without taking them into account for new measurements, this issue was solved and the weld bead width could be monitored constantly.

With the possibility of doing reliable online measurement of the bead width, some research and development possibilities are created. Future works will be done focusing on mapping the bead width online during and entire layer builds, when adjacent beads will be presented in the image. Also an algorithm for automatically verifying the deviation, pointing areas where the presence of defects would be higher with the support of deep learning can be developed using this work as base.

REFERENCES

Buades, A., Coll, B., and Morel, J.M. (2011). Non-Local Means Denoising. *Image Processing On Line*, 1, 208–212.

Canny, J. (1986). A Computational Approach to Edge Detection. *IEEE Transactions on Pattern Analysis and Machine Intelligence*, PAMI-8(6), 679–698.

Chen, S., Qiu, T., Lin, T., Wu, L., Tian, J., Lv, W., and Zhang, Y. (2004). Intelligent Technologies for Robotic Welding. In *Robotic Welding, Intelligence and Automation*, 123–143. Springer.

Chen, X.Z., Chen, S.B., and Lin, T. (2007). Recognition of Macroscopic Seam for Complex Robotic Welding Environment. In *Robotic Welding, Intelligence and Automation*, volume 362, 171–178. Springer.

Chu, H.H. and Wang, Z.Y. (2016). A vision-based system for post-welding quality measurement and defect detection. *The International Journal of Advanced Manufacturing Technology*, 86, 3007–3014.

Cruz, J.G., Torres, E.M., and Absi Alfaro, S.C. (2015). A methodology for modeling and control of weld bead width in the GMAW process. *Journal of the Brazilian Society of Mechanical Sciences and Engineering*, 37, 1529–1541.

Ding, D., Pan, Z., Cuiuri, D., and Li, H. (2015a). A multi-bead overlapping model for robotic wire and arc additive manufacturing (WAAM). *Robotics and Computer-Integrated Manufacturing*, 31, 101–110.

Ding, D., Pan, Z., Cuiuri, D., and Li, H. (2015b). Wire-feed additive manufacturing of metal components: technologies, developments and future interests. *The International Journal of Advanced Manufacturing Technology*, 81, 465–481.

Ding, D., Pan, Z., Cuiuri, D., Li, H., van Duin, S., and Larkin, N. (2016). Bead modelling and implementation of adaptive MAT path in wire and arc additive manufacturing. *Robotics and Computer-Integrated Manufacturing*, 39, 32–42.

Ding, J., Colegrove, P., Mehnen, J., Ganguly, S., Sequeira Almeida, P., Wang, F., and Williams, S. (2011). Thermo-mechanical analysis of Wire and Arc Additive Layer Manufacturing process on large multi-layer parts. *Computational Materials Science*, 50, 3315–3322.

Font comas, T., Diao, C., Ding, J., Williams, S., and Zhao, Y. (2017). A Passive Imaging System for Geometry Measurement for the Plasma Arc Welding Process. *IEEE Transactions on Industrial Electronics*, 64(9), 7201–7209. doi:10.1109/TIE.2017.2686349.

Gibson, I., Rosen, D.W., and Stucker, B. (2010). *Additive Manufacturing Technologies*. Springer US.

Gonzalez, R.C. and Woods, R.E. (2007). *Digital Image Processing (3rd Edition)*. Pearson.

Pinto-Lopera, J.E., Motta, J.M.S., and Alfaro, S.C.A. (2016). Real-time measurement of width and height of weld beads in GMAW processes. *Sensors (Switzerland)*, 16, 1–14. doi:10.3390/s16091500.

Williams, S.W., Martina, F., Addison, A.C., Ding, J., Pardal, G., and Colegrove, P. (2016). Wire + Arc Additive Manufacturing. *Materials Science and Technology*, 32, 641–647.

Wu, B., Pan, Z., Ding, D., Cuiuri, D., Li, H., Xu, J., and Norrish, J. (2018). A review of the wire arc additive manufacturing of metals: properties, defects and quality improvement. *Journal of Manufacturing Processes*, 35, 127–139.

Wu, J. and Chen, S.B. (2007). Software System Designs of Real-Time Image Processing of Weld Pool Dynamic Characteristics. In *Robotic Welding, Intelligence and Automation*, volume 362, 303–309. Springer.

Xiong, J., Zhang, G., Gao, H., and Wu, L. (2013a). Modeling of bead section profile and overlapping beads with experimental validation for robotic GMAW-based rapid manufacturing. *Robotics and Computer-Integrated Manufacturing*, 29, 417–423.

Xiong, J., Zhang, G., Qiu, Z., and Li, Y. (2013b). Vision-sensing and bead width control of a single-bead multi-layer part: material and energy savings in GMAW-based rapid manufacturing. *Journal of Cleaner Production*, 41, 82–88.

Xu, Y., Fang, G., Chen, S., Zou, J.J., and Ye, Z. (2014). Real-time image processing for vision-based weld seam tracking in robotic GMAW. *The International Journal of Advanced Manufacturing Technology*, 73, 1413–1425. doi:10.1007/s00170-014-5925-1.

Xu, Y., Lv, N., Fang, G., Du, S., Zhao, W., Ye, Z., and Chen, S. (2017). Welding seam tracking in robotic gas metal arc welding. *Journal of Materials Processing Technology*, 248, 18–30. doi:10.1016/j.jmatprotec.2017.04.025.

Yuan Li, You Fu Li, Qing Lin Wang, De Xu, and Min Tan (2010). Measurement and Defect Detection of the Weld Bead Based on Online Vision Inspection. *IEEE Transactions on Instrumentation and Measurement*, 59, 1841–1849.